IOPscience iopscience.iop.org

Home Search Collections Journals About Contact us My IOPscience

Modulation instability and dissipative ion-acoustic structures in collisional nonthermal electron-positron-ion plasma: solitary and shock waves

This content has been downloaded from IOPscience. Please scroll down to see the full text.

2016 Plasma Sources Sci. Technol. 25 055006

(http://iopscience.iop.org/0963-0252/25/5/055006)

View the table of contents for this issue, or go to the journal homepage for more

Download details:

IP Address: 202.117.62.134
This content was downloaded on 11/08/2016 at 01:45

Please note that terms and conditions apply.

IOP Publishing Plasma Sources Science and Technology

Plasma Sources Sci. Technol. **25** (2016) 055006 (11pp) doi:10.1088/0963-0252/25/5/055006

Modulation instability and dissipative ion-acoustic structures in collisional nonthermal electron-positron-ion plasma: solitary and shock waves[5]

Shimin Guo[1,6], Liquan Mei[1], Ya-Ling He[2], Chenchen Ma[3] and Youfa Sun[4]

[1] School of Mathematics and Statistics, Xi'an Jiaotong University, Xi'an 710049, People's Republic of China
[2] Key Laboratory of Thermo-Fluid Science and Engineering of Ministry of Education, Xi'an Jiaotong University, Xi'an 710049, People's Republic of China
[3] School of Electrical Engineering, Xi'an Jiaotong University, Xi'an 710049, People's Republic of China
[4] School of Economics and Commerce, Guangdong University of Technology, Guangzhou 510520, People's Republic of China

E-mail: gsm861@126.com

Received 24 January 2016, revised 15 April 2016
Accepted for publication 20 June 2016
Published 10 August 2016

Abstract

The nonlinear behavior of an ion-acoustic wave packet is investigated in a three-component plasma consisting of warm ions, nonthermal electrons and positrons. The nonthermal components are assumed to be inertialess and hot where they are modeled by the kappa distribution. The relevant processes, including the kinematic viscosity amongst the plasma constituents and the collision between ions and neutrals, are taken into consideration. It is shown that the dynamics of the modulated ion-acoustic wave is governed by the generalized complex Ginzburg–Landau equation with a linear dissipative term. The dispersion relation and modulation instability criterion for the generalized complex Ginzburg–Landau equation are investigated numerically. In the general dissipation regime, the effect of the plasma parameters on the dissipative solitary (dissipative soliton) and shock waves is also discussed in detail.

Keywords: electron-positron-ion plasma, ion-acoustic wave, generalized complex Ginzburg–Landau equation, modulation instability

(Some figures may appear in colour only in the online journal)

1. Introduction

In recent years, the study of electron-positron-ion (EPI) plasma has seen an explosive growth because of its potential applications in astrophysical environments and in laboratory experiments [1–6]. For example, the positrons can be created in an interstellar medium when the cosmic-ray nuclei interact with atoms [7, 8]. This means that the EPI plasma can be considered as an omnipresent ingredient of several astrophysical situations such as the active galactic nuclei [9], solar atmospheres [10], fireballs producing gamma-ray bursts [11], etc. In the laboratory, such a three-component plasma has been created by using the positrons as probes to investigate transport in Tokamak [12]. On the other hand, there is a growing experimental interest in generating electron-positron plasmas in controlled laboratory environments [13–16].

Because of the importance of EPI plasma, the study of a low frequency wave named 'ion-acoustic wave' in such plasma system has become a hot topic providing a better understanding

[5] The project is supported by NSF of China (11501441, 11371289, 11371288), National Natural Science Foundation of China (U1261112), China Postdoctoral Science Foundation (2014M560756), and Fundamental Research Funds for the Central Universities (xjj2015067).
[6] Author to whom any correspondence should addressed.

 © 2016 IOP Publishing Ltd Printed in the UK

of nonlinear phenomena in both astrophysical and laboratory conditions [3, 17, 18, 19–22]. Though the annihilation of electrons and positrons exists in the EPI plasma, it can be shown that the annihilation time in such plasma is sufficiently long for the collective interaction to take place [23]. In laboratory, the electron-positron plasma with charge neutrality (same amount of matter and antimatter), high-density ($n_e, n_p \simeq 10^{16}$ cm^3) and small divergence has been successfully produced, where the spatial distribution of the electron-positron plasma propagating through the background electron-ion plasma has been investigated [13]. This work opens up the possibility of studying the collective behavior in electron-positron plasma, which indicates that the ion-acoustic waves can exit in the EPI plasma in the sense that the electron-positron lifetime is much larger than the characteristic time scale for collective oscillations [24].

It is well known that the nonlinear structures of ion-acoustic wave are pronouncedly affected by the velocity distribution of the charged particles in plasmas. Generally speaking, the Maxwellian distribution is proper to analyze the wave motions in the plasma environments where memories and microscopic interactions are short ranged. The astrophysical plasmas are generally subject to spatial or temporal long-range interactions evolving in a non-Euclidean, multifractal space-time, which leads to residing in non-equilibrium stationary states. In some cases of in situ observations, nonthermal electrons have been also found in the near-Earth space plasmas. For modeling such plasmas, an appropriate particle distribution function is the so-called kappa (κ) distribution function introduced by Vasyliunas [25]. The energetic particles (electrons and positrons in our model) populate the superthermal region of the velocity distribution [26, 27], and thus result in a high-energy tail in the distribution function. This distribution presents a good fit to the data from satellite [28–31] and laboratory experiments [32–34]. Some examples are as follows: in [30], the authors found that the kappa distribution with $\kappa = 2.70$ is consistent with mean electron spectra producing hard x-ray emission of solar flares. Maksimovic *et al* [31] developed a Lorentzian ion exosphere model with $\kappa = 4$ yielding good agreement with electron distributions observed in the solar wind. In the laboratory, the kappa distribution was employed in experimental studies of electron holes [34]. Note that though the links between the kappa distribution and the Tsallis nonextensive formalism [35, 36] have been discussed recently, this analogy is still a controversial topic.

One of the interesting research fields is the nonlinear structures in the form of wave packets which have been observed in space plasmas [37], in the laboratory experiments [38], and in numerical simulations [39]. These electrostatic structures can be interpreted by modulation instability (MI) which may occur due to the nonlinear self-interaction of the carrier waves, parametric wave coupling, or interaction between high- and low-frequency modes [40]. By the inclusion of dissipative effect, the plasma is no longer Hamiltonian but is the dissipative system. The canonical paradigm of an evolution equation, governing the dynamics of a slowly varying wave packet envelope in the dissipative system, is the complex Ginzburg–Landau (CGL) type equation (nonlinear Schrödinger equation with complex coefficients). The analytical solutions of CGL type equation have been addressed including dissipative solitons, shocks, breathing pulses, and holes [41–43].

The aim of this paper is to investigate the nonlinear dynamics of modulated ion-acoustic wave packets in a dissipative EPI plasma, taking into account the effect of kinematic viscosity of the ion fluids, collision between ion and neutrals as well as superthermal electrons and positrons featuring kappa distribution, etc. Considering various effects can give a much more complete picture in the EPI plasma. A detailed understanding of nonlinear wave processes sustained by such a plasma is of fundamental importance. The runaway electrons and positrons have been investigated by many authors recently [44–46]. It is worth studying the effect of runaway electrons and positrons on the nonlinear waves in plasma, although it is beyond the scope of the paper here. In fact, in order to pinpoint the building blocks of a more realistic and complete EPI plasma model, using a simple model for the first approach is part of our scope. Therefore, our work can be considered as the preliminary research.

The paper is organized as follows. In section 2, we present the Euler–Poisson system for our dissipative EPI plasma. In section 3, the generalized CGL equation governing the evolution of the ion-acoustic wave packets is derived by employing the multiscale perturbation analysis. In section 4, we present the MI analysis of the dissipative ion-acoustic waves. In addition, the nonlinear structures of dissipative solitary and shock waves are investigated for the generalized CGL equation. Finally, the concluding remarks are given in section 5.

2. Theoretical model and basic equations

We consider the nonlinear propagation of the ion-acoustic wave in a one-dimensional, unmagnetized, and collisional EPI plasma, whose components are ions, superthermal electrons and positrons. In our plasma model, the ion component is treated as a classical plasma fluid, while the electrons and positrons are considered as a fast neutralizing background. The ions are taken to be viscous and warm, where the kinematic viscosity and pressure terms are contained in the ion-momentum equation. In addition, the electron and positron inertia can in fact be neglected because the phase velocity of ion-acoustic wave is much lower than the thermal speeds of these two species, which implies that we do not need to take the general fluid equations for electrons and positrons. This is also a requirement for Landau damping to be minimized [47]. Furthermore, the superthermal electrons and positrons are assumed to obey the kappa distribution. The Euler–Poisson system for the nonlinear dynamics of ion-acoustic wave in our EPI plasma is described as follows.

The normalized ion dynamic equations, i.e. the continuity and momentum equations, are written as,

$$\frac{\partial n_i}{\partial t} + \frac{\partial (n_i u_i)}{\partial x} = 0, \tag{1}$$

$$\frac{\partial u_i}{\partial t} + u_i \frac{\partial u_i}{\partial x} + \gamma \sigma n_i \frac{\partial n_i}{\partial x} = -\frac{\partial \varphi}{\partial x} + \eta \frac{\partial^2 u_i}{\partial x^2} - \nu u_i. \tag{2}$$

Integrating the kappa distribution function over the velocity space, we obtain the normalized electron and positron densities as follows [48]

$$n_{\mathrm{e}} = \left(1 - \frac{\varphi}{\kappa_{\mathrm{e}} - 3/2}\right)^{-\kappa_{\mathrm{e}}+1/2}, \tag{3}$$

$$n_{\mathrm{p}} = \left(1 + \delta\frac{\varphi}{\kappa_{\mathrm{p}} - 3/2}\right)^{-\kappa_{\mathrm{p}}+1/2}. \tag{4}$$

The spectral indices κ_{e} and κ_{p} in the above two equations, measuring the slope of the energy spectrum of the superthermal electrons and positrons, form the high-energy tail in the velocity distribution function. The smaller values of κ_{e} and κ_{p} denote the stronger superthermality of electrons and positrons, respectively. The kappa distribution, in the limit $\kappa_{\mathrm{e}}, \kappa_{\mathrm{p}} \to +\infty$, degenerates into the well-known Maxwellian distribution. Note that the condition $\kappa_{\mathrm{e}}, \kappa_{\mathrm{p}} > 3/2$ is required for a physically meaningful thermal speed.

The above four equations are coupled through the following Poisson equation

$$\frac{\partial\varphi^2}{\partial x^2} = n_{\mathrm{e}} - \alpha n_i - \beta n_{\mathrm{p}}. \tag{5}$$

Equations (1)–(5) form a closed system governing the dynamics of ion-acoustic wave in the collisional viscous EPI plasma with superthermal electrons and positrons. In these equations, the space x and time t are normalized by the Debye length $\lambda_{\mathrm{D}} = (\kappa_{\mathrm{B}}T_{\mathrm{e}}/4\pi n_{\mathrm{i}0}e^2)^{1/2}$ and the inverse ion plasma frequency $\omega_i^{-1} = (4\pi n_{\mathrm{i}0}e^2/m_i)^{-1/2}$, respectively. Also, n_j ($j = i$, e, or p for ions, electrons, or positrons, respectively) denotes the number density of each species normalized by the equilibrium value n_{j0}, u_i stands for the ion fluid velocity normalized by ion sound velocity $C_i = (\kappa_{\mathrm{B}}T_{\mathrm{e}}/m_i)^{1/2}$, φ is the electric potential normalized by $\kappa_{\mathrm{B}}T_{\mathrm{e}}/e$, η is the kinematic viscosity normalized by $\lambda_{\mathrm{D}}^2\omega_i$, $\sigma = T_i/T_{\mathrm{e}}$, $\delta = T_{\mathrm{e}}/T_{\mathrm{p}}$. Here, T_j ($j = i$, e, or p) denotes the temperature of each species, e is the electronic charge, κ_{B} the Boltzmann constant, m_i the ion mass. The physical quantity $\gamma = (N+2)/N$ represents the adiabatic constant where N is the number of degrees of freedom. For our one-dimensional EPI plasma, we have $N = 1$, and accordingly $\gamma = 3$. From the overall quasi-neutrality condition $n_{\mathrm{e}0} = n_{\mathrm{i}0} + n_{\mathrm{p}0}$, we have $1 = \alpha + \beta$ with $\alpha = n_{\mathrm{i}0}/n_{\mathrm{e}0}$ and $\beta = n_{\mathrm{p}0}/n_{\mathrm{e}0}$. The last term $-\nu u_i$ in the right side of the ion-momentum equation (2) denotes the change of ion fluid velocity through the collisions with neutrals, the parameter ν is the collisional frequency normalized by ω_i.

Note that in the limiting case of no ions (the pure electron-positron plasma), equations (1) and (2) should be removed from our theoretical model. And then, the assumption of neglecting the electron and positron inertia is also invalid. Therefore, we can see that our theoretical model could not present the results in the limiting case of no ions.

3. Generalized complex Ginzburg–Landau equation

In this section, we use the multiscale perturbation analysis [49] to derive the generalized CGL equation governing the dynamics of a slowly varying amplitude (envelope) of ion-acoustic wave near the equilibrium state.

Let the vector $S = (n_i, u_i, \varphi)$ stand for the state of the system at a given position x and time t, $\epsilon(\ll 1)$ be a dimensionless and small parameter. Introducing the stretched space and time variables

$$X_n = \epsilon^n x,\ T_n = \epsilon^n t,\ \ n = 0, 1, 2, \cdots,$$

we expand the state of the system around the equilibrium state $S^{(0)} = (1, 0, 0)$ as

$$S = S^{(0)} + \sum_{n=-\infty}^{n=+\infty}\sum_{l=-\infty}^{l=+\infty} \epsilon^n S_l^{(n)}(X_{n\geqslant 1}, T_{n\geqslant 1})\mathrm{e}^{\mathrm{i}l(kx-\omega t)}, \tag{6}$$

where $i^2 = -1$, the real variables k and ω denote the wave number and angular frequency of the wave packet, respectively. Because the physical quantities n_i, u_i, and φ are real, the reality condition $S_{-1}^{(n)} = S_l^{(n)*}$ is required to be satisfied. Here the asterisk represents the complex conjugate. Since the collision frequency between ions and neutrals is small compared to the ion oscillation frequency, we assume that $\nu \sim O(\epsilon^2)$ in the following calculations.

By substituting the ansatz (6) into the Euler–Poisson system (1)–(5) and collecting the terms of the same power of ϵ, we obtain a set of reduced equations for the lth harmonic mode. For the equations with $n = 1$ and $l = 1$, we obtain the first harmonic components of the number density and fluid velocity expressed in the following matrix form

$$\begin{pmatrix} n_{i1}^{(1)} \\ u_{i1}^{(1)} \end{pmatrix} = \begin{pmatrix} \dfrac{-\mathrm{i}k^2}{3\mathrm{i}\sigma k^2 - \mathrm{i}\omega^2 + \omega\eta k^2} \\ \dfrac{-\mathrm{i}k\omega}{3\mathrm{i}\sigma k^2 - \mathrm{i}\omega^2 + \omega\eta k^2} \end{pmatrix}\varphi_1^{(1)}, \tag{7}$$

with the compatibility condition

$$\omega^2 + \mathrm{i}\eta k^2\omega - \frac{k^2(-3\beta d_1\sigma + \alpha + 3c_1\sigma + 3\sigma k^2)}{c_1 + k^2 - \beta d_1} = 0, \tag{8}$$

Here $c_1 = (2\kappa_{\mathrm{e}} - 1)/(2\kappa_{\mathrm{e}} - 3)$, $d_1 = -(2\kappa_{\mathrm{p}} - 1)\delta/(2\kappa_{\mathrm{p}} - 3)$. The above equation (8) is the linear dispersion relation for ion-acoustic wave in our EPI plasma. If we neglect the kinematic viscosity of the plasma, i.e. $\eta = 0$, the linear dispersion relation (8) reduces to $\omega^2 - \frac{k^2(-3\beta d_1\sigma + \alpha + 3c_1\sigma + 3\sigma k^2)}{c_1 + k^2 - \beta d_1} = 0$, which coincides with equation (12) in [50].

Obviously, the linear dispersion relation (8) for our viscous EPI plasma has two complex roots for real values of wave number k. The real part $\mathrm{Re}(\omega)$ of ω represents the ion-acoustic wave frequency, while the imaginary part $\mathrm{Im}(\omega)$ stands for the damping rate of the wave. From figure 1, we can see that the variation of $\mathrm{Re}(\omega)$ with wave number k is affected by the

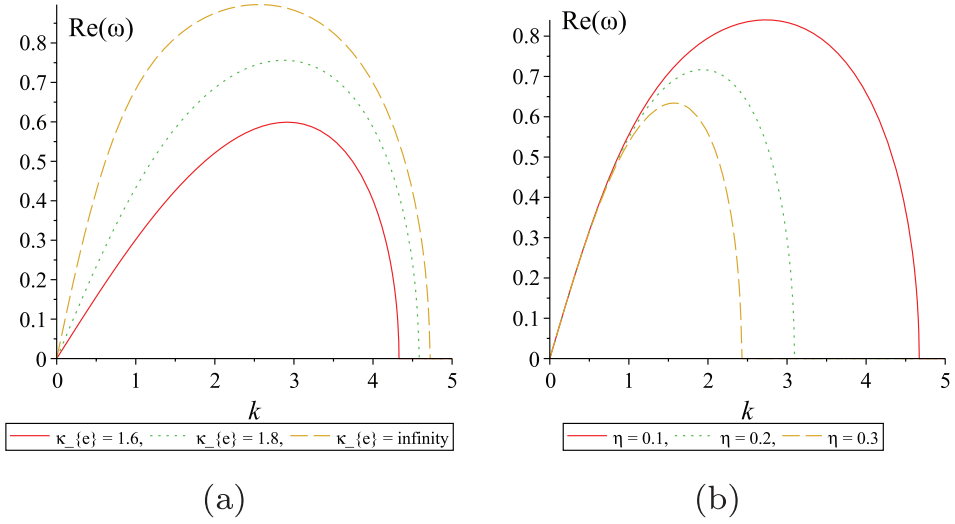

Figure 1. The variation of real frequency Re(ω) versus wave number k for different values of spectral index κ_e (a) and kinematic viscosity η (b). The parameters are $\alpha = 0.95$, $\delta = 1$, $\sigma = 0.005$, $\kappa_p = 2.7$, (a): $\eta = 0.1$, (b): $\kappa_e = 2.4$.

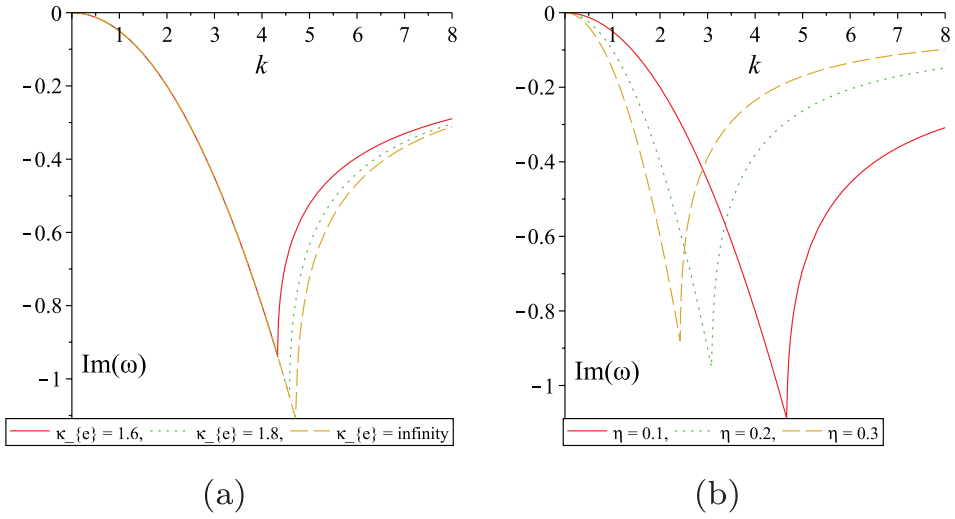

Figure 2. The variation of imaginary frequency Im(ω) versus wave number k for different values of spectral index κ_e (a) and kinematic viscosity η (b). The parameters are the same as in figure 1.

spectral index of electrons κ_e and kinematic viscosity η. Plot (a) shows that the values of Re(ω) increase with an increase of κ_e, where the Maxwellian distribution is approached. This is due to the fact that the non-thermality of the particles leads to a reduction of the plasma screening length. As is depicted in plot (b), the opposite effect can be found for an increasing value of kinematic viscosity η, i.e. increasing the kinematic viscosity of the dissipative media leads to a reduction in the ion-acoustic wave frequency. The damping rate of ion-acoustic wave, i.e. the imaginary part of the frequency, is numerically investigated in figure 2. Clearly, Im(ω) is always negative. Plot (a) reveals that increasing κ_e value slightly decreases the damping rate. It can be seen from plot (b) that increasing η leads to a reduction of damping rate until k approaches a certain value k_c, while an increase of η increases the damping rate if $k > k_c$. The spectral index of positrons κ_p has the same qualitative behavior on Re(ω) and Im(ω) as in figures 1 and 2, respectively. For simplicity, we do not present the results here.

The second order ($n = 2$) reduced equations with $l = 1$ yields the following solvability condition

$$\frac{\partial \varphi_1^{(1)}}{\partial T_1} + V\frac{\partial \varphi_1^{(1)}}{\partial X_1} = 0. \tag{9}$$

Here V is the complex group velocity of ion-acoustic wave packets expressed as

$$V = \frac{\partial \omega}{\partial k} = \frac{f_1}{f_2}, \tag{10}$$

where

$$\begin{aligned} f_1 &= 2k(-3\mathrm{i}\beta d_1\sigma - \beta d_1\omega\eta + 6\mathrm{i}k^2\sigma - \mathrm{i}\omega^2 + 2k^2\omega\eta + 3\mathrm{i}c_1\sigma \\ &\quad + c_1\omega\eta + \mathrm{i}\alpha), \\ f_2 &= -2\mathrm{i}\beta d_1\omega + \beta d_1\eta k^2 + 2\mathrm{i}k^2\omega - k^4\eta + 2\mathrm{i}c_1\omega - c_1\eta k^2. \end{aligned}$$

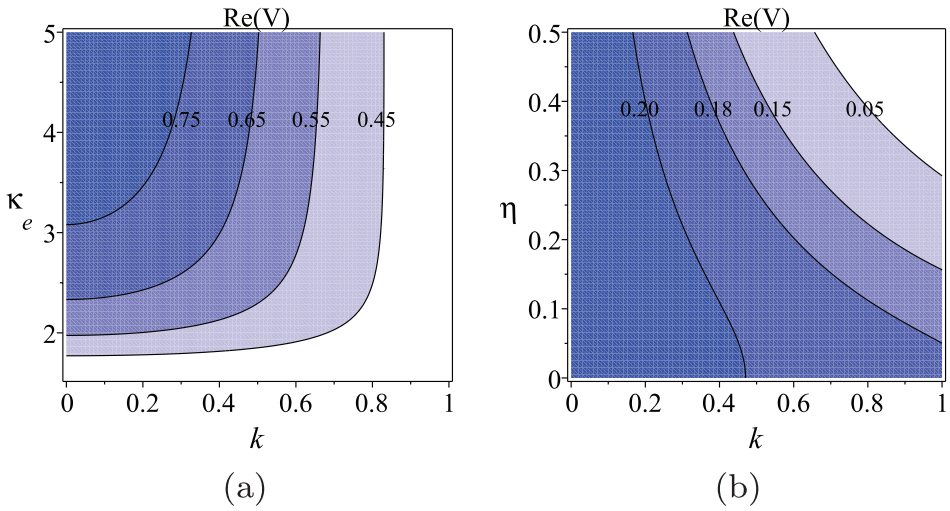

Figure 3. The contour of the real part of group velocity $\mathrm{Re}(V)$ on the (κ_e, k)- and (η, k)-planes. The parameters are $\alpha = 0.96$, $\delta = 0.9$, $\sigma = 0.001$, $\kappa_p = 2.4$, (a): $\eta = 0.15$, (b): $\kappa_e = 2.7$.

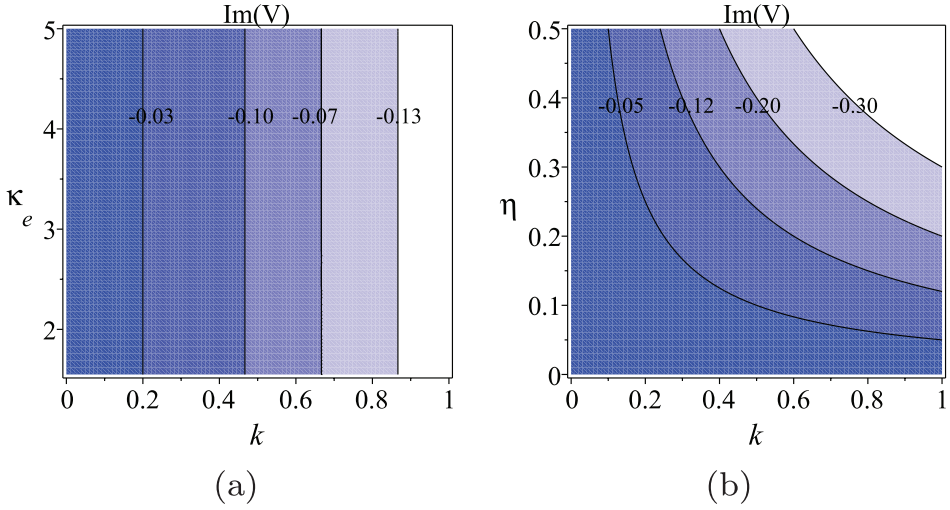

Figure 4. The contour of the imaginary part of group velocity $\mathrm{Im}(V)$ on the (κ_e, k)- and (η, k)-planes. The parameters are the same as in figure 3.

In the absence of kinematic viscosity ($\eta = 0$), equation (10) reduces to $V = \frac{k(3\beta d_1\sigma - 6\sigma k^2 + \omega^2 - 3c_1\sigma - \alpha)}{\omega(\beta d_1 - k^2 - c_1)}$, which recovers the group velocity expressed in equation (14) in [50] for the conservative nonthermal EPI plasma. It is obvious from equation (10) that the group velocity in a viscous plasma, generally speaking, is complex. The real part $\mathrm{Re}(V)$ of group velocity is related to the physical group velocity [51], while the imaginary part $\mathrm{Im}(V)$ represents the slow drift of the central wave number along the wave packet trajectory [52]. The parametric investigation of $\mathrm{Re}(V)$ and $\mathrm{Im}(V)$ is presented in figures 3 and 4, respectively. It is clear that increasing κ_e leads to an increase of the real part of the group velocity, as is depicted in figure 3 (a). While $\mathrm{Re}(V)$ is a decreasing function of η, as is shown in figure 3 (b). Figure 4 indicates that the imaginary part of the group velocity takes negative values. It is evident that the spectral index of electrons κ_e does not affect the imaginary part of the group velocity $\mathrm{Im}(V)$, while it is seen that increasing η makes the $\mathrm{Im}(V)$ become lower. We speculate such behavior is due to the fact that the plasma system dissipates more wave energy for higher kinematic viscosity.

The second-harmonic modes ($n = l = 2$), generating from the nonlinear self-interaction of the carrier waves, can be obtained in terms of $(\varphi_1^{(1)})^2$ as

$$\begin{pmatrix} n_{i2}^{(2)} \\ u_{i2}^{(2)} \\ \varphi_2^{(2)} \end{pmatrix} = \begin{pmatrix} \Delta_1 \\ \Delta_2 \\ \Delta_3 \end{pmatrix} (\varphi_1^{(1)})^2, \tag{11}$$

where the expressions for Δ_1, Δ_2, and Δ_3 are given in the appendix.

The reduced equations for the zeroth harmonic components $l = 0$ at the third order $n = 3$ are

$$\begin{pmatrix} n_{i0}^{(2)} \\ u_{i0}^{(2)} \\ \varphi_0^{(2)} \end{pmatrix} = \begin{pmatrix} \Delta_4 \\ \Delta_5 \\ \Delta_6 \end{pmatrix} \left|\varphi_1^{(1)}\right|^2, \tag{12}$$

where Δ_4, Δ_5, and Δ_6 are given in the appendix.

Finally, the third harmonic modes ($n = 3$, $l = 1$) with the aid of equations (7), (9), (11), and (12) yield an explicit compatibility condition in the form of the generalized CGL equation

$$\mathrm{i}\left(\frac{\partial \Phi}{\partial T_2} + V\frac{\partial \Phi}{\partial X_2}\right) + P\frac{\partial^2 \Phi}{\partial X_1^2} + Q|\Phi|^2\Phi + \mathrm{i}\Upsilon\Phi = 0 \tag{13}$$

where $\Phi = \varphi_1^{(1)}$, the dispersion coefficient $P(=\mathrm{Re}(P) + \mathrm{iIm}(P))$, the nonlinear coefficient $Q(=\mathrm{Re}(Q) + \mathrm{iIm}(Q))$, and the linear gain/loss coefficient $\Upsilon(=\mathrm{Re}(\Upsilon) + \mathrm{iIm}(\Upsilon))$ are

$$\begin{aligned}
P &= \frac{1}{2}\frac{\partial^2\omega}{\partial k^2} = \frac{\mathrm{i}}{\alpha k^2 \mathcal{B}}[\mathrm{i}\mathcal{A}\omega^4 + (2\,\alpha V k - 2\mathcal{A}\eta\, k^2 + 3\mathrm{i}\alpha\eta k^2)\omega^3 \\
&\quad + (-\mathrm{i}\mathcal{A}\alpha - 3\mathrm{i}\alpha k^3\eta V - \mathrm{i}\mathcal{A}\eta^2 k^4 - 9\alpha\sigma\, k^2 - 3\alpha V^2 k^2 \\
&\quad - 6\mathrm{i}\mathcal{A}\sigma\, k^2 + \alpha k^4\eta^2)\omega^2 + (-\mathcal{A}\alpha\, k^2\eta + 6\mathrm{i}\alpha\, k^4\eta\sigma \\
&\quad + 18\alpha V k^3\sigma + 2\mathrm{i}\mathcal{A}\alpha V k + \alpha V k^5\eta^2 - 3\mathrm{i}\alpha V^2 k^4\eta \\
&\quad + 6\mathcal{A}k^4\sigma\,\eta)\omega - 3\alpha k^4 V^2\sigma - \mathcal{A}\alpha V k^3\eta + 9\mathrm{i}\mathcal{A}k^4\sigma^2 \\
&\quad - 9\alpha k^4\sigma^2 + 3\mathrm{i}\alpha k^5\eta V\sigma - 3\mathrm{i}\mathcal{A}\alpha k^2\sigma + \alpha V^2 k^6\eta^2], \\
Q &= \frac{\mathrm{i}}{\alpha k^2\mathcal{A}^2\mathcal{B}}[(2\mathrm{i}\alpha k^4\omega^3\eta + \alpha k^2\omega^4 - 9\alpha k^6\sigma^2 \\
&\quad - \alpha k^6\omega^2\eta^2)(\Delta_1 + \Delta_4) + (-\alpha k^7\eta^2\omega - 6\alpha k^5\omega\sigma \\
&\quad + 2\alpha k^3\omega^3 + 3\mathrm{i}\alpha k^5\omega^2\eta - 3\mathrm{i}\alpha k^7\eta\sigma)(\Delta_2 + \Delta_5) \\
&\quad + \mathcal{A}(c_2 - \beta d_2)(-2\mathrm{i}\omega^4 + 4\eta k^2\omega^3 + (2\mathrm{i}\eta^2 k^4 + 12\mathrm{i}k^2\sigma)\omega^2 \\
&\quad - 12\sigma\eta k^4\omega - 18\mathrm{i}k^4\sigma^2)(\Delta_3 + \Delta_6)], \\
\Upsilon &= \frac{\nu\omega\mathcal{A}}{\mathcal{B}}.
\end{aligned}$$

Here, $\mathcal{A}$ and $\mathcal{B}$ are given in the appendix.

By introducing the Galilean transformation

$$\begin{aligned}
\xi &= \frac{1}{\epsilon}(X_2 - VT_2) = (X_1 - VT_1) = \epsilon(x - Vt), \\
\tau &= T_2 = \epsilon T_1 = \epsilon^2 t,
\end{aligned}$$

the nonlinear evolution equation (13) becomes

$$\mathrm{i}\frac{\partial \Phi}{\partial \tau} + P\frac{\partial^2 \Phi}{\partial \xi^2} + Q|\Phi|^2\Phi + \mathrm{i}\Upsilon\Phi = 0. \tag{14}$$

The above generalized CGL equation governs the dynamic of the amplitude associated with ion-acoustic wave packets in viscous collisional EPI plasma, where the appearance of the linear dissipative term $\mathrm{i}\Upsilon\Phi$ is due to the collision between ions and neutrals. If we neglect the ion-neutral collision ($\nu = 0$), the generalized CGL equation (14) reduces to the well-known cubic complex Ginzburg–Landau equation [58].

4. Modulation instability and dissipative waves

The physical phenomena giving the nonlinearity, which is introduced by the choice of the generalized CGL equation (14), include the modulation instability, the dissipative solitary wave, and the dissipative shock wave. In this section, we study the MI of ion-acoustic wave at short wavelengths and investigate the nonlinear structures of dissipative ion-acoustic wave in the EPI plasma.

4.1. Modulation instability

Because of the collision between ions and neutrals, we assume that the plane wave solution of equation (14) possesses the following form

$$\Phi(\tau, \xi) = \Phi_0(\tau)\exp\left(-\mathrm{i}\int_0^\tau \Delta(\tau)\mathrm{d}\tau\right), \tag{15}$$

where $\Phi_0(\tau)$ is the amplitude of the pump carrier wave, $\Delta(\tau)$ is the nonlinear frequency shift in the presence of linear dissipative term. Substitution of equation (15) into equation (14) yields

$$\begin{aligned}
&\frac{\mathrm{d}\Phi_0(\tau)}{\mathrm{d}\tau} + \Upsilon\Phi_0(\tau) = 0 \Rightarrow \Phi_0(\tau) = \Phi_{00}\exp(-\Upsilon\tau), \\
&\Delta(\tau) = -Q|\Phi_0(\tau)|^2 = -Q|\Phi_{00}|^2\exp(-2\Upsilon\tau),
\end{aligned}$$

where Φ_{00} is a real constant.

To investigate the MI of ion-acoustic wave in our EPI plasma, we split the amplitude Φ into two parts

$$\Phi = (\Phi_0(\tau) + \psi(\tau, \xi))\exp\left(-\mathrm{i}\int_0^\tau \Delta(\tau)\mathrm{d}\tau\right), \tag{16}$$

where $\psi(|\psi| \ll \Phi_0)$ is the small-amplitude perturbation. Substituting equation (16) into equation (14) and linearizing the result with respect to ψ, we obtain the following evolution equation for the perturbation

$$\mathrm{i}\frac{\partial \psi}{\partial \tau} + P\frac{\partial^2 \psi}{\partial \xi^2} + Q|\Phi_0|^2(\psi + \psi^*) + \mathrm{i}\Upsilon\psi = 0, \tag{17}$$

where ψ^* is the complex conjugate of ψ.

Substituting the perturbation $\psi(\tau, \xi) = U\mathrm{e}^{\mathrm{i}(K\xi - \Omega\tau)} + V\mathrm{e}^{-\mathrm{i}(K\xi - \Omega^*\tau)}$ into equation (16), we obtain the following Lange and Newell's criterion [53, 54] after the mathematical manipulation:

The ion-acoustic wave is unstable (i.e. supercritical) for

$$\mathrm{Re}(P)\mathrm{Re}(Q) + \mathrm{Im}(P)\mathrm{Im}(Q) > 0,$$

while it is stable (i.e. subcritical) for

$$\mathrm{Re}(P)\mathrm{Re}(Q) + \mathrm{Im}(P)\mathrm{Im}(Q) < 0.$$

Here, U and V are complex constants, $K(|K| \ll k)$ and $\Omega\,(|\Omega| \ll \omega)$ are the modulation wave number and frequency, respectively.

Based on the above findings, it can be seen that the parametric investigation of MI is of great importance. The effect of the plasma parameters on the sign of $\mathrm{Re}(P)\mathrm{Re}(Q) + \mathrm{Im}(P)\mathrm{Im}(Q)$, which determines where the stable and unstable regions set

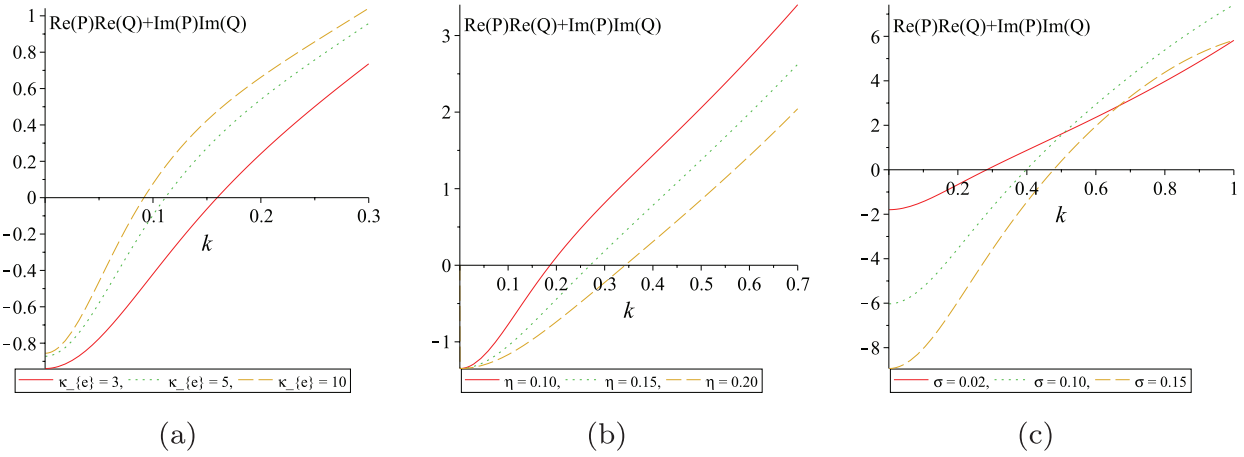

Figure 5. The curves of $\mathrm{Re}(P)\mathrm{Re}(Q) + \mathrm{Im}(P)\mathrm{Im}(Q)$ versus k for different values of κ_e (a), η (b), and σ (c). The parameters are $\alpha = 0.95$, $\delta = 1$, $\kappa_p = 3$, (a): $\eta = 0.15$, $\sigma = 0.01$, (b): $\kappa_e = 2$, $\sigma = 0.01$, (c): $\eta = 0.15$, $\kappa_e = 2$.

in, is depicted in figure 5. From plot (a), we can see that an increase of the spectral index of electrons κ_e leads to a decrease of the critical wave number threshold k_c for which $\mathrm{Re}(P)\mathrm{Re}(Q) + \mathrm{Im}(P)\mathrm{Im}(Q)$ changes its sign, where the unstable (stable) region becomes wider (narrower). This means that the superthermality of electrons can result in the shrinkage of the instability, which changes the unstable case into the stable case. To study the effect of ion kinematic viscosity η and the ratio of ion temperature to electron temperature σ on MI, we present the variations of $\mathrm{Re}(P)\mathrm{Re}(Q) + \mathrm{Im}(P)\mathrm{Im}(Q)$ in plots (b) and (c), respectively. Clearly, increasing η and σ leads to a reduction of the instability regime and an increase of the stable domain. This means that the kinematic viscosity can dissipate the energy of our EPI plasma and lead to a restraint upon the instability of the wave packets, which makes stable domain wider for larger η. Moreover, it is expected that the unstable region is wider in the EPI plasma with warm ions ($\sigma > 0$) than that in the EPI plasma with cold ions ($\sigma = 0$).

In the limiting case of no viscosity, i.e. $\eta = 0$, the generalized CGL equation (14) reduces to the following damped nonlinear Schrödinger (NLS) equation with real coefficients

$$\mathrm{i}\frac{\partial \Phi}{\partial \tau} + \widehat{P}\frac{\partial^2 \Phi}{\partial \xi^2} + \widehat{Q}|\Phi|^2\Phi + \mathrm{i}\widehat{\Upsilon}\Phi = 0, \tag{18}$$

where $\widehat{P} = \mathrm{Re}(P)$, $\widehat{Q} = \mathrm{Re}(Q)$, and $\widehat{\Upsilon} = \mathrm{Re}(\Upsilon)$. According to the Lange and Newell's criterion, we can see the above equation is stable for $\widehat{P}\widehat{Q} < 0$ where the ion-acoustic wave can propagate in the form of dark-type excitations. If $\widehat{P}\widehat{Q} > 0$, the amplitude modulated envelope is unstable for $K \leqslant K_c = 2Q|\Phi_0|^2/P$ due to the external perturbations. In this case, the bright-type wave packets can be generated in the plasma system.

4.2. Dissipative solitary and shock waves

In the non-conservative plasma, the dissipative soliton can be generated due to the counterbalance between loss and gain terms, in addition to the balance between the nonlinear and dispersion effects. Furthermore, the shock-type waves can be created in the dissipative media because of the interplay between the dispersion and dissipation effects.

4.2.1. Dissipative solitary waves. Inspired to the work in [55, 57], the dissipative solitary wave solution of the generalized CGL equation (14) is

$$\Phi(\xi, \tau) = \rho \mathrm{sech}^{1-i\mu}(\lambda\xi)\exp(-\mathrm{i}\theta\tau), \tag{19}$$

where

$$\begin{aligned}
\rho^2 &= \frac{\lambda^2}{\mathrm{Re}(Q)}[(2-\mu)\mathrm{Re}(P) + 3\mu\mathrm{Im}(P)],\\
\mu &= -\zeta \pm \sqrt{2+\zeta^2},\\
\lambda^2 &= \frac{\mathrm{Re}(\Upsilon)}{\mathrm{Im}(P) - 2\mu\mathrm{Re}(P) - \mu^2\mathrm{Im}(P)},\\
\zeta &= \frac{3(\mathrm{Re}(P)\mathrm{Re}(Q) + \mathrm{Im}(P)\mathrm{Im}(Q))}{2(\mathrm{Im}(P)\mathrm{Re}(Q) - \mathrm{Re}(P)\mathrm{Im}(Q))},\\
\theta &= \lambda^2[(\mu^2-1)\mathrm{Re}(P) - 2\mu\mathrm{Im}(P)] - \mathrm{Im}(\Upsilon).
\end{aligned}$$

Here, ρ is the amplitude of solitary wave, μ represents the chirp parameter, λ is the inverse width of the solitary wave, θ is the frequency associated with the nonlinear phase shift.

The influence of the plasma parameters including the ratio of ion temperature to electron temperature σ, the kinematic viscosity η, the collisional frequency ν, and the spectral index of positrons κ_p on the dissipative solitary wave structure is studied in figure 6. One can see from plot (a) that the amplitude of the dissipative solitary wave increases with an increase of σ, while the width of the wave is a decreasing function of σ. Therefore, dissipative solitary waves in the EPI plasma with cold ions ($\sigma = 0$) are expected to have a smaller amplitude and broader width than that in the EPI plasma with warm ions. Plot (b) exhibits that both the amplitude and width of the dissipative solitary wave increase when kinematic viscosity increases, which reveals that an increase in η leads to an enhancement of the nonlinearity of the system and makes the pulses taller. As is apparent from

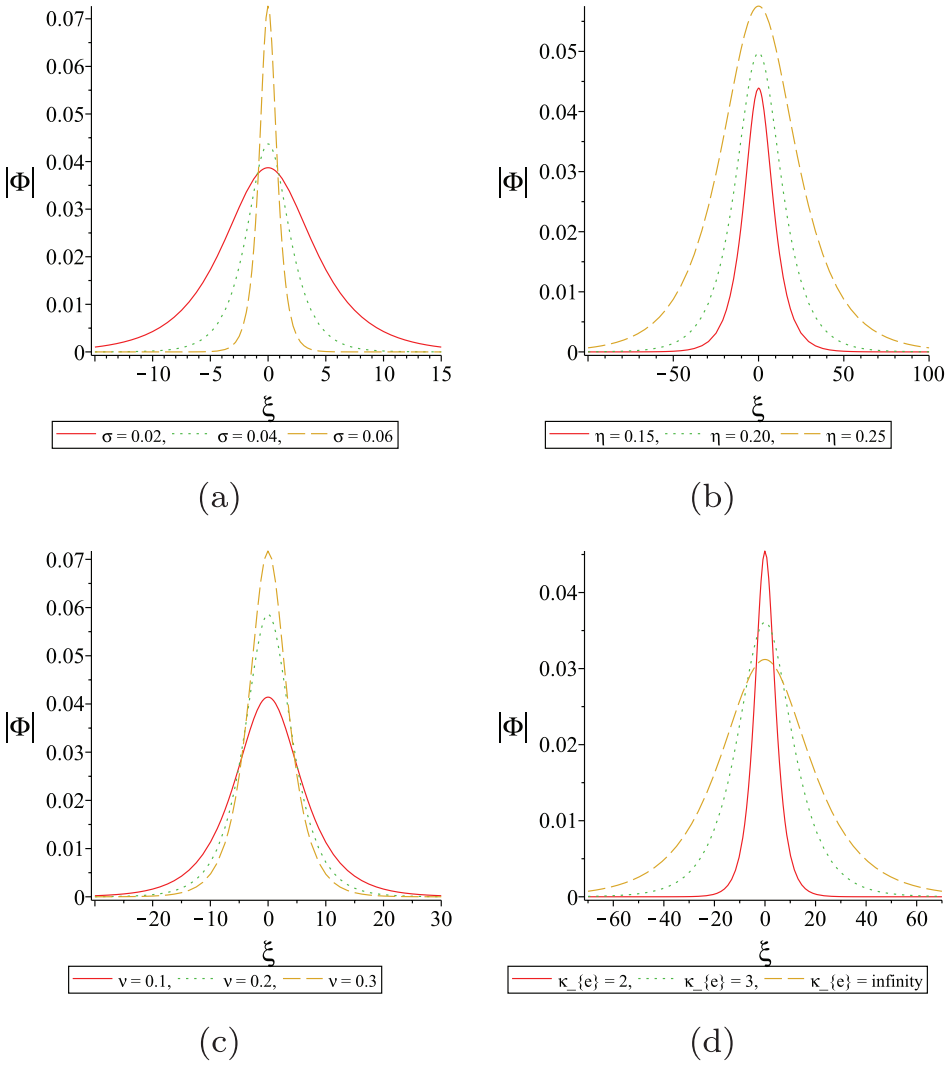

Figure 6. The absolute values of the electrostatic potential Φ expressed by equation (19) for different values of σ (a), η (b), ν (c), and κ_e (d). The parameters are $\alpha = 0.95$, $\delta = 1$, $\kappa_p = 3.5$, $k = 1.8$ (a): $\eta = 0.1$, $\nu = 0.1$, $\kappa_e = 2.2$, (b): $\sigma = 0.01$, $\nu = 0.1$, $\kappa_e = 2.2$, (c): $\sigma = 0.01$, $\eta = 0.1$, $\kappa_e = 2.2$, (d): $\sigma = 0.01$, $\eta = 0.1$, $\nu = 0.1$.

plot (c), an increase of collisional frequency ν leads to the formation of a taller but narrower dissipative solitary wave in the EPI plasma. Plot (d) shows that when the spectral index of electrons κ_e increases, the amplitude of dissipative solitary wave decreases. In other words, a stronger superthermality of the plasma can concentrate a significant amount of energy in the system and therefore the pulses become taller. Thus, the dissipative solitary wave with a taller amplitude is expected to be in the superthermal plasma than that in the Maxwellian plasma.

4.2.2. Dissipative shock waves. In addition to the dissipative solitary waves, the generalized CGL equation (14) admits the following shock wave solution as well [56]

$$\Phi(\xi,\tau) = \frac{\rho e^{-\lambda(\xi-c\tau)}}{(1+e^{-\lambda(\xi-c\tau)})^{1+i\mu}} \exp i(\chi\xi - \theta\tau), \qquad (20)$$

where the parameters satisfy the following relations

$$\begin{aligned}
\rho^2 &= \frac{\mathrm{Im}(P)(\chi+\mu\lambda)^2 + \mathrm{Re}(\Upsilon)}{\mathrm{Im}(Q)},\\
\chi &= -\frac{3\lambda \mathrm{Re}(P)}{2\mathrm{Im}(P)},\ c = \frac{-3\lambda(\mathrm{Re}(P)^2 + \mathrm{Im}(P)^2)}{\mathrm{Im}(P)},\\
\mu &= -\zeta \pm \sqrt{2+\zeta^2},\\
\theta &= -\mu\lambda c + \mathrm{Re}(P)(\chi+\mu\lambda)^2 - \mathrm{Re}(Q)\rho^2 - \mathrm{Im}(\Upsilon),\\
\lambda^2 &= -\frac{4\varrho \mathrm{Re}(\Upsilon)\mathrm{Im}(P)}{\mathrm{Im}(P)\mathrm{Im}(Q) + \varrho(-3\mathrm{Re}(P) + 2\mu\mathrm{Im}(P))^2},\\
\varrho &= \frac{\mathrm{Re}(P)\mathrm{Re}(Q) + \mathrm{Im}(P)\mathrm{Im}(Q)}{(2-\mu^2)(\mathrm{Re}(P)^2 + \mathrm{Im}(P)^2)},\\
\zeta &= \frac{3(\mathrm{Re}(P)\mathrm{Re}(Q) + \mathrm{Im}(P)\mathrm{Im}(Q))}{2(\mathrm{Re}(P)\mathrm{Im}(Q) - \mathrm{Im}(P)\mathrm{Re}(Q))}.
\end{aligned}$$

The solution (20) represents the shock wave propagating in our EPI plasma, where ρ is the amplitude of the shock, μ the chirp parameter, c the velocity of the shock wave in the moving reference frame, χ and θ stand for the wave number

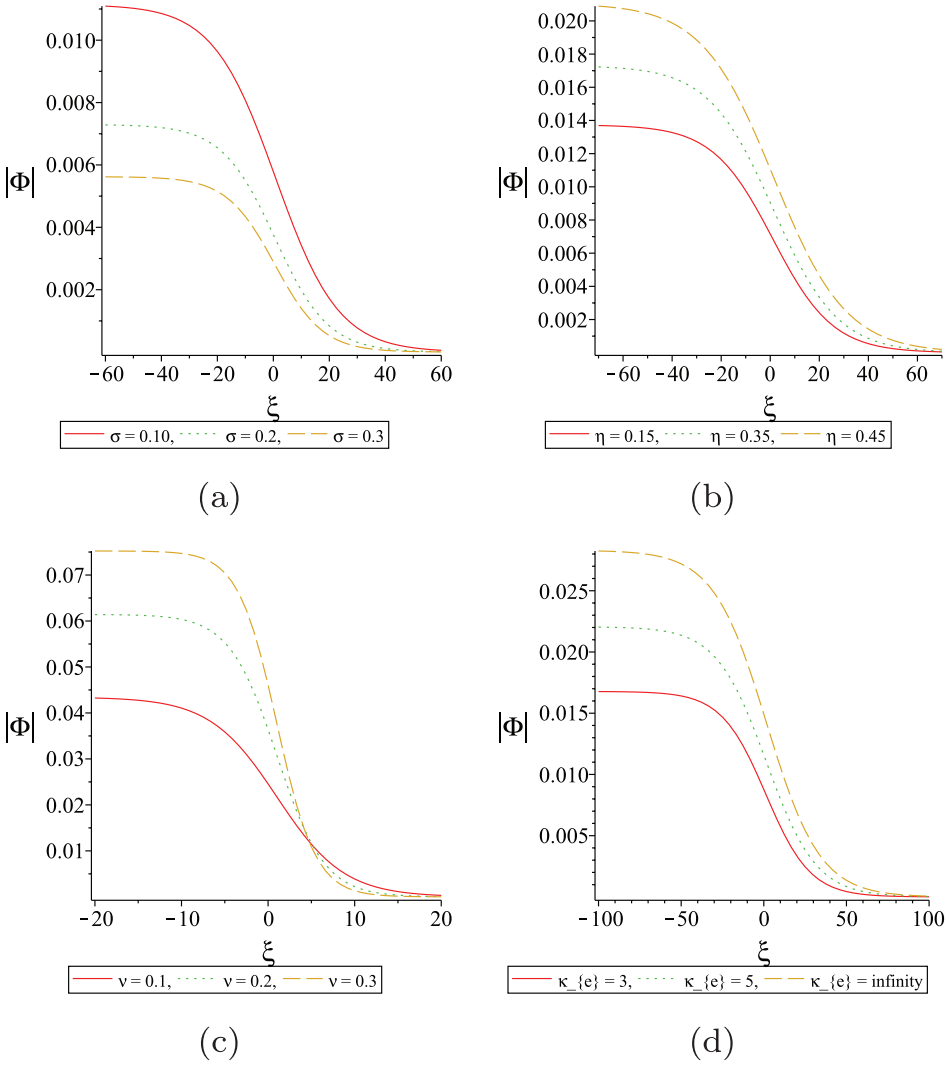

Figure 7. Variations of the dissipative shock waves with respect to ξ for different values of σ (a), η (b), ν (c), and κ_e (d). The parameters are $\alpha = 1, \delta = 1, \kappa_p = 1.8, k = 1$ (a): $\eta = 0.15, \nu = 0.01, \kappa_e = 2.5$, (b): $\sigma = 0.1, \nu = 0.01, \kappa_e = 2.5$, (c): $\sigma = 0.1, \eta = 0.15, \kappa_e = 2.5$, (d): $\sigma = 0.1, \eta = 0.15, \nu = 0.1$.

and angular frequency associated with the nonlinear phase shift, respectively.

In [26], the authors investigated the ion-acoustic shock waves in the superthermal plasmas with no positron in the long-wave approximation. Here, we discuss the nonlinear features of dissipative shock waves in the limit case of no positron in the short-wave approximation.

As is clearly shown in figure 7, the electrostatic shock profile can be significantly affected by the plasma parameters including the ratio of ion temperature to electron temperature σ, kinematic viscosity η, the collisional frequency ν, and the spectral index of electrons κ_e. From plot (a), we can see that both the potential and steepness of the dissipative shock wave decrease with an increase of σ. This means that the stronger dissipative shock wave is expected to be generated in the EPI plasma with cold ions, i.e. $\sigma = 0$. It is observed in plots (b), (c), and (d) that when the values of η, ν and κ_e increase, the amplitude of the dissipative shock wave increases and become steeper. Therefore, it can be indicated that the stronger dissipative shock wave can occur in the dissipative EPI plasma with stronger viscosity, weaker superthermality, and stronger collision effects. In comparison with the nonthermal EPI plasma, a stronger dissipative shock structure with a larger amplitude is expected to be created in the EPI plasmas with thermal electrons.

5. Conclusions

To summarize, we investigate the nonlinear propagation of ion-acoustic wave in a viscous collisional electron-positron-ion plasma whose components are warm ions and kappa distributed electrons and positrons. Due to the presence of the dissipative effect (ion kinematic viscosity and ion-neutral collision), the evolution of the ion-acoustic wave envelope is governed by the generalized complex Ginzburg–Landau equation with a linear dissipative term, which is a model equation for the non-integrable system.

We find that both the angular frequency and group velocity of the wave packet have real and imaginary components, where their variations with relevant plasma parameters including spectral index and kinematic viscosity are numerically investigated. Furthermore, it is found that the region of the MI of the ion-acoustic wave becomes narrower with the increase of ion kinematic viscosity η and the ratio of ion temperature to electron temperature σ, while the MI region becomes wider when the spectral index of electrons κ_e increases. Then we investigate the effect of the plasma parameters on the profile of dissipative solitary and shock waves. It is discovered that the increase in the values of σ and ν (collisional frequency) leads to the formation of taller but narrower dissipative solitary waves in EPI plasmas, while both the amplitude and width of the dissipative solitary waves increase when the values of η increase. In addition, a stronger superthermality of electrons can concentrate a significant amount of energy of the EPI plasma, which makes the amplitude of dissipative solitary waves taller. On the other hand, when the kinematic viscosity and collisional frequency increase, both the amplitude and steepness of the dissipative shock wave increases. It reveals that a stronger dissipative shock wave can be created in a viscous collisional EPI plasma. An increase of σ leads to the formation of shorter and wider dissipative shock waves, while increasing κ_e value leads to an increase of the amplitude of the waves.

Our theoretical investigation can be helpful in understanding nonlinear features of dissipative ion-acoustic wave in the non-Hamiltonian EPI plasma. Because a detailed investigation of non-thermality in EPI plasma is of fundamental importance in a wide range of applications from astrophysical plasmas to laboratory experiments, our investigation can also provide a better understanding of the relations between the non-thermal electrons and space and laboratory plasmas. In addition, the present work establishes a connection between the dissipative plasma dynamics and generalized complex Ginzburg–Landau equation, which provides new theoretical models in plasma physics.

Acknowledgments

The authors express their sincere thanks to the editor and referees for their valuable comments which led to an improved version. We also thank Professor Dr R Sabry for useful discussions.

Appendix. Expressions of the coefficients

$$\Delta_1 = -\frac{k^4(c_1-\beta d_1+4k^2)(3\omega^2+4\mathrm{i}k^2\eta\omega+3k^2\sigma)-k^2\mathcal{A}^2(\beta d_2-c_2)}{2[(c_1-\beta d_1+4k^2)(\omega^2+2\mathrm{i}k^2\eta\omega-3\sigma k^2)-k^2\alpha]},$$

$$\Delta_2 = -\frac{k\omega[(c_1-\beta d_1+4k^2)(k^2\omega^2+9k^4\sigma)+2\alpha k^4+2\mathcal{A}^2(c_2-\beta d_2)]}{2[(c_1-\beta d_1+4k^2)(\omega^2+2\mathrm{i}k^2\eta\omega-3\sigma k^2)-k^2\alpha]},$$

$$\begin{aligned}\Delta_3 = &-\frac{1}{2[(c_1-\beta d_1+4k^2)(\omega^2+2\mathrm{i}k^2\eta\omega-3\sigma k^2)-k^2\alpha]}\\ &\times[(3\alpha k^4+2c_2\mathcal{A}^2-2\beta d_2\mathcal{A}^2)\omega^2\\ &+4\mathrm{i}\eta k^2(k^2\alpha+c_2\mathcal{A}^2-\beta d_2\mathcal{A}^2)\omega\\ &-3\sigma k^2(k^4\alpha+2\beta d_2\mathcal{A}^2-2c_2\mathcal{A}^2)],\end{aligned}$$

$$\Delta_4 = -\frac{2k^3\omega}{V},$$

$$\Delta_5 = -\frac{k^2(\omega^2V+6\sigma k\omega+3\sigma k^2V)}{V^2},$$

$$\Delta_6 = -\frac{2(-\beta d_2V\mathcal{A}^2+c_2V\mathcal{A}^2+\alpha k^3\omega)}{V(-\beta d_1+c_1)},$$

$$\mathcal{A} = k^2\omega\eta+3\mathrm{i}k^2\sigma-\mathrm{i}\omega^2,$$

$$\mathcal{B} = 6\mathrm{i}k^2\omega\sigma-3k^4\eta\sigma+3k^2\eta\omega^2+\mathrm{i}k^4\eta^2\omega-2\mathrm{i}\omega^3.$$

References

[1] Chen H, Wilks S C, Bonlie J D, Liang E P, Myatt J, Price D F, Meyerhofer D D and Beiersdorfer P 2009 *Phys. Rev. Lett.* **102** 105001
[2] Cheng L, Tang R, Zhang A and Xue J 2013 *Phys. Rev.* E **87** 025101
[3] Sabry R, Moslem W M, Shukla P K and Saleem H 2009 *Phys. Rev.* E **79** 056402
[4] Ferdousi M, Sultana S and Mamun A A 2015 *Phys. Plasmas* **22** 032117
[5] Lee M J and Jung Y D 2015 *Plasma Sources Sci. Technol.* **24** 032001
[6] de Urquijo J 2010 *Plasma Sources Sci. Technol. The 29th Int. Conf. on Phenomena in Ionized Gases (July, 2009)*
[7] El-Awady E I, El-Tantawy S A, Moslem W M and Shukla P K 2010 *Phys. Lett.* A **374** 3216
[8] Adriani O *et al* 2009 *Nature* **458** 607
[9] Miller H R and Witta P J 1998 *Active Galactic Nuclei* (Berlin: Springer)
[10] Tandberg-Hansen E and Emshie A G 1988 *The Physics of Solar Flares* (Cambridge: Cambridge University Press) p 124
[11] Piran T 1999 *Phys. Rep.* **314** 575
[12] Tinkle M D, Greaves R G, Surko C M, Spencer R L and Mason G W 1994 *Phys. Rev. Lett.* **72** 352
[13] Sarri G *et al* 2015 *Nat. Commun.* **6** 6747
[14] Sarri G *et al* 2013 *Phys. Rev. Lett.* **110** 255002
[15] Chen H *et al* 2015 *Phys. Rev. Lett.* **114** 215001
[16] Chen H *et al* 2010 *Phys. Rev. Lett.* **105** 015003
[17] Rasheed A, Murtaza G and Tsintsadze N L 2010 *Phys. Rev.* E **82** 016403
[18] Salahuddin M, Saleem H and Saddiq M 2002 *Phys. Rev.* E **66** 036407
[19] El-Tantawy S A and Moslem W M 2014 *Phys. Plasmas* **21** 052112
[20] Adnan M, Mahmood S and Qamar A 2014 *Phys. Plasmas* **21** 092119
[21] Uddin M J, Alam M S and Mamun A A 2015 *Phys. Plasmas* **22** 022111
[22] Guo S, Mei L and Sun A 2013 *Ann. Phys.* **332** 38
[23] Saleem H, Haque Q and Vranješ J 2003 *Phys. Rev.* E **67** 057402

[24] Misra A P and Samanta S 2010 *Phys. Rev.* E **82** 037401
[25] Vasyliunas V M 1968 *J. Geophys. Res.* **73** 2839
[26] Sultana S, Sarri G and Kourakis I 2012 *Phys. Plasmas* **19** 012310
[27] Guo S, Mei L and Shi W 2013 *Phys. Lett.* A **377** 2118
[28] Gloeckler G and Fisk L A 2006 *Astrophys. J. Lett.* **648** L63
[29] Sarri G *et al* 2010 *Phys. Plasmas* **17** 010701
[30] Kašparová J and Karlický M 2009 *Astron. Astrophys.* **497** L13
[31] Maksimovic M, Pierrard V and Lemaire J F 1997 *Astron. Astrophys.* **324** 725
[32] Yagi Y, Antoni V, Bagatin M, Desideri D, Martines E, Serianni G and Vallone F 1997 *Plasma Phys. Control. Fusion* **39** 1915
[33] Magni S, Roman H E, Barni R, Riccardi C, Pierre T and Guyomarc D 2005 *Phys. Rev.* E **72** 026403
[34] Goldman M V, Newman D L and Mangeney A 2007 *Phys. Rev. Lett.* **99** 145002
[35] Renyi A 1955 *Acta Math. Acad. Sci. Hung.* **6** 285
[36] Tsallis C 1988 *J. Stat. Phys.* **52** 479
[37] Pottelette R, Ergun R E, Treumann R A, Berthomier M, Carlson C W, McFadden J P and Roth I 1999 *Geophys. Res. Lett.* **26** 2629
[38] Depierreux S, Fuchs J, Labaune C, Michard A, Baldis H A, Pesme D, Hüller S and Laval G 2000 *Phys. Rev. Lett.* **84** 2869
[39] Cohen B I, Lasinski B F, Langdon A B and Williams E A 1997 *Phys. Plasmas* **4** 956
[40] Borhanian J 2013 *Plasma Phys. Control. Fusion* **55** 105012
[41] Descalzi O 2005 *Phys. Rev.* E **72** 046210
[42] Afanasjev V V, Akhmediev N and Soto-Crespo J M 1996 *Phys. Rev.* E **53** 1931
[43] Gutiérrez P, Escaff D, Pérez-Oyarzún S and Descalzi O 2009 *Phys. Rev.* E **80** 037202
[44] Petrović Z Lj *et al J. Phys. D: Appl. Phys.* **42** 194002
[45] Banković A *et al New J. Phys.* **14** 035003
[46] Vrhovac S B, Stojanović V D, Jelenković B M and Petrović Z Lj *J. Appl. Phys.* **90** 5871
[47] Mace R L, Amery G and Hellberg M A 1999 *Phys. Plasmas* **6** 44
[48] Baluku T K and Hellberg M A 2008 *Phys. Plasmas* **15** 123705
[49] Taniuti T and Yajima J M P N 1969 *J. Math. Phys.* **10** 1369
[50] Akhtar N, Mahmood S and Siddiqui S 2014 *Plasma Phys. Control. Fusion* **56** 095027
[51] Tokman M D, Westerhofand E and Gavrilova M A 2003 *Nucl. Fusion* **43** 1295
[52] Muschiettiand L and Dum C T 1993 *Phys. Fluids* B **5** 1383
[53] Lange C G and Newell A C 1974 *SIAM J. Appl. Math.* **27** 441
[54] Pelap F B and Faye M M 2005 *Phys. Scr.* **71** 238
[55] Stenflo L, Yu M Y and Shukla P K 1989 *Phys. Scr.* **40** 257
[56] Yomba E, Kofané T C and Pelap F B 1996 *J. Phys. Soc. Japan* **65** 2337
[57] Dai C Q, Cen X and Wu S S 2008 *Comput. Math. Appl.* **56** 55
[58] Aranson I S and Kramer L 2002 *Rev. Mod. Phys.* **74** 99